

# Obscured AGN Population and its Evolution

Yuichi Terashima<sup>1</sup>

<sup>1</sup> Ehime University, Matsuyama, Ehime 790-8577, Japan  
*E-mail(YT): terasima@astro.phys.sci.ehime-u.ac.jp*

## ABSTRACT

Recent results from *Suzaku* observations of obscured active galactic nuclei (AGN) and implications for their evolution are presented. We utilize *Suzaku* data to measure broad-band spectra of obscured AGN selected by [OIII] $\lambda$ 5007 optical emission lines or hard X-rays, and to constrain the structure of the nucleus. Spectra of obscured AGNs are well represented by a canonical model consisting of absorbed and unabsorbed power laws, a reflection continuum, an Fe-K line, and soft emission lines in most cases. We derive the distribution of absorption column densities for the [OIII] selected sample and find that about a half are Compton-thick, supporting earlier results with better quality of data. Some of hard X-ray selected obscured AGNs show very weak soft emission, which is presumed to be scattered by photoionized gas in the opening part of the absorber. The weakness of the scattered emission suggests that they are buried in a geometrically thick absorber. In order to explore such a new type of AGNs, we also present results on a new sample of obscured AGNs selected from the XMM-Newton serendipitous source catalogue and compare the geometry of obscuring matter and various fundamental parameters.

KEY WORDS: galaxies:active — X-rays:galaxies

## 1. Introduction

Obscured AGNs constitute a significant fraction of AGNs and are an essential class of objects in many aspects of AGN studies including unification and evolution of AGNs, relationship to their host galaxies, and the origin of the Cosmic X-ray background. X-ray observations have played a key role in untangling the nature of obscured AGN population since the discovery of “hidden Seyfert 1 nuclei” in Seyfert 2s, supporting a unified model of AGNs (Awaki et al. 1990). Subsequent observations have shown that their X-ray spectra consist of absorbed power law accompanied by a strong Fe-K line, soft X-ray emission scattered by ionized gas in the opening part of the obscuring matter, soft X-rays produced by starburst activity, and so on. Broad-band X-ray observations are a powerful way to decompose such complicated spectra and to measure the amount of absorption/reflection, intrinsic power, and so on (e.g., Done et al. 1996). Since the combination of these components depends on the geometry of the obscuring matter, measurements of the spectral components can be used to constrain the structure of obscuring matter.

Although well selected samples are clearly required for thorough understanding of this population, constructing unbiased samples of obscured AGNs, however, is difficult because of large absorption. Optical narrow emission lines like [OIII] $\lambda$ 5007 and hard X-rays are less affected by absorption and are often employed as a measure of

intrinsic power of AGNs and a means to define AGN samples in a less biased manner. We have been conducting systematic *Suzaku* observations of obscured AGNs selected by different methods. In this paper, we summarize results from *Suzaku* observations of AGNs selected by means of optical emission lines and hard X-rays with *Swift* BAT. We also present a study of obscured AGNs in the *XMM-Newton* archives to extend our results from *Suzaku* and to discuss implications for the evolution of obscured AGNs. Objects in our samples are mostly in the local universe, which can be basis of understanding high- $z$  objects and AGN evolution.

## 2. Optical Emission-line Selected Sample

[OIII] $\lambda$ 5007 optical narrow emission lines are often used as a tracer of intrinsic luminosity of AGNs. Risaliti et al. (1999) defined an [OIII] flux limited sample selected from Seyfert 1.8, 1.9, and 2 galaxies in the Revised Shapley Ames catalog (Maiolino & Rieke 1995) and studied the distribution of absorbing column densities ( $N_{\text{H}}$ ), which is a fundamental input for population synthesis models of the Cosmic X-ray background. About a half of their sample are Compton-thick and their X-ray emission below  $\sim 10$  keV is substantially attenuated. X-ray spectra above 10 keV for some of the Compton-thick objects have been measured with *BeppoSAX*, while many objects have not been observed at hard X-rays or only upper limits on the hard X-ray fluxes have been obtained, for which

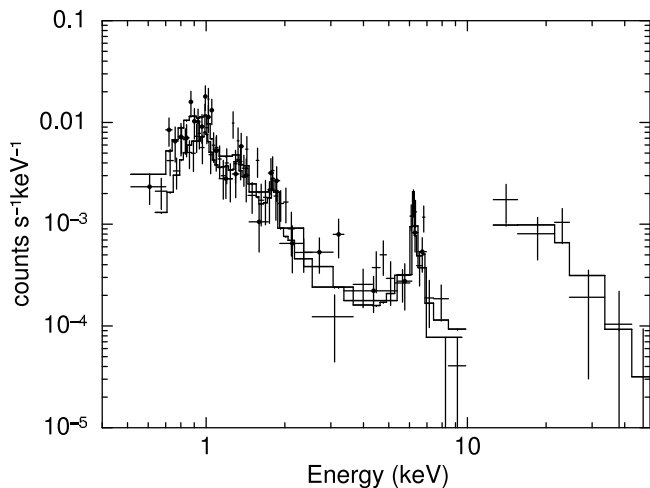


Fig. 1. *Suzaku* spectra of the Seyfert 2 Mrk 1073 in [OIII]-selected sample fitted with the canonical model.

measurements of  $N_{\text{H}}$  are ambiguous.

We selected objects bright in [OIII] and without high quality hard X-ray data from Risaliti’s sample and observed them with *Suzaku* for typical exposures of 40 ksec to measure their broad band spectral shape. One object NGC 4968, which is a Seyfert 2 very bright in [OIII] but not included in Risaliti’s sample, was also observed. We observed 11 Seyfert 2s in total and high quality data are available for 35 [OIII] brightest objects if observations with *Suzaku*, *BeppoSAX*, *XMM-Newton* for the rest of Risaliti’s sample are combined.

All the objects in our sample are clearly detected with the XIS, while hard X-rays above 15 keV are detected from seven objects with the HXD/PIN. The spectra of our sample are well explained by a “canonical” model consisting of an absorbed power law, an unabsorbed power law, soft plasma emission, a reflection continuum, and strong Fe-K emission. The photon indices for both absorbed and unabsorbed power laws were fixed at 1.9 in our fits.  $N_{\text{H}}$  values are reasonably constrained for our sample except for five objects, for which only lower limits on  $N_{\text{H}}$  were obtained. The best-fit  $N_{\text{H}}$  values are in the range  $(1-5) \times 10^{24} \text{ cm}^{-2}$ , although  $N_{\text{H}}$  values depend on assumed strength and absorption of the reflection continuum. All the objects show strong Fe-K line emission at around 6.4 keV. The *Suzaku* spectra of the Seyfert 2 Mrk 1073 is shown in Figure 1 as an example. The distribution of  $N_{\text{H}}$  is shown in Figure 2 (Awaki et al. 2010). About a half of the objects are Compton-thick, confirming the results obtained by Risaliti et al. with better quality broad band data.

Hard X-ray surveys above 10 keV can detect more heavily absorbed AGNs compared to surveys at lower energies. The distribution of column densities measured for *Swift*/BAT and *INTEGRAL* selected AGN samples

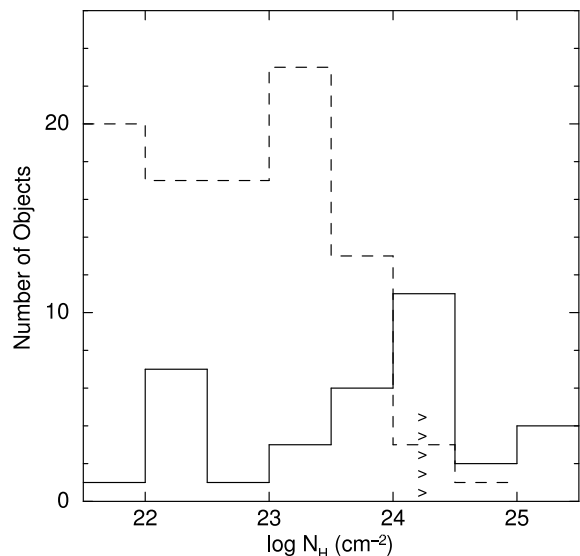


Fig. 2. Distribution of absorption column densities for [OIII] (solid line) and *Swift*/BAT (dashed line) selected samples. The “>” symbol denotes lower limits on  $N_{\text{H}}$  in the [OIII] sample. The data for the *Swift* sample are taken from Tueller et al. (2008) and contain both unobscured and obscured AGN.

are published in, e.g., Tueller et al. (2008) and Malizia et al. (2009), respectively. The  $N_{\text{H}}$  distribution for the Tueller et al. sample is also shown in Figure 2 as a dashed line. The number of AGNs with  $N_{\text{H}}$  greater than  $1 \times 10^{24} \text{ cm}^{-2}$  is very limited in the hard X-ray samples and these surveys are likely to be still biased against objects with  $N_{\text{H}} > 10^{24} \text{ cm}^{-2}$ .

### 3. Monte Carlo Simulation of Expected Spectra

We have developed a ray-tracing Monte-Carlo simulation code to predict X-ray spectra from obscured AGNs by assuming a torus-shaped cold absorber surrounding a nucleus as shown in Figure 3 (Ikeda et al. 2009). The incident spectra from the nucleus is assumed to be a power law with an exponential cutoff at 360 keV, and photoelectric absorption and Compton scattering inside the absorber are taken into account. Our model can calculate three components (transmission, unabsorbed reflection, and absorbed reflection) separately. Since the shape and the strength of these components depend on the geometry of the absorber, parameters in our model (opening angle, inclination angle viewed from the observer, and column density along the equatorial plane) can be constrained from comparison with observed spectral shape.

Figure 4 is an example of application of our model to the *Suzaku* spectrum of the Seyfert 2 NGC 2273 (Awaki et al. 2009). Absorbed reflection, unabsorbed reflection, and transmitted components are shown as dot-dashed, dashed, and dotted lines in this figure, respectively. The

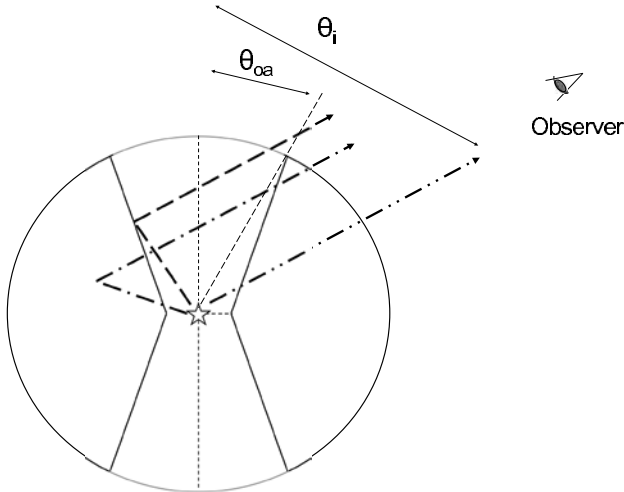


Fig. 3. Geometry of obscuring matter assumed in our simulations. Dashed-, dot-dashed, and dot-dot-dashed lines represent unabsorbed reflection, absorbed reflection, and transmitted components, respectively.  $\theta_i$  is the inclination angle and  $\theta_{oa}$  is the half opening angle.

spectrum below 10 keV is dominated by an unabsorbed reflection component. This means that the inner wall of the other side of the torus is visible and that the inclination angle is close to the opening angle. The  $N_H$  value along the equatorial plane of  $\sim 5 \times 10^{24} \text{ cm}^{-2}$  was obtained and the opening angle was not tightly constrained. Application of our model to the Seyfert 2 Mrk 3 is discussed in Ikeda et al. (2009) and analysis of more objects is ongoing.

#### 4. *Swift*/BAT AGN: Discovery of a New Type of Buried AGNs

Since the *Swift*/BAT instrument is sensitive at hard X-rays (15–150 keV) and has a large field view (2 sr), a hard X-ray all sky survey is possible (Markwardt et al. 2005, Tueller et al. 2008). We have been conducting *Suzaku* follow up observations of BAT selected AGNs.

Figure 5 shows the *Suzaku* spectrum of one of BAT selected AGNs Swift J1238.9–2720 (ESO 506–G027). This spectrum is represented by a combination of absorbed and unabsorbed power laws, a reflection continuum, and a strong Fe-K emission line (detailed results of this object is presented in Winter et al. 2009b). It is clear from comparison with Figure 1 that the strength of the soft X-ray emission relative to hard emission in this object is much weaker than that in Mrk 1073, which is an [OIII] bright Seyfert 2. The possible origins of soft X-ray emission are photoionized gas irradiated by AGN radiation and thermal gas produced by starburst activity. *Chandra* and *XMM-Newton* grating observations have shown that, in at least several Seyfert 2s, soft emission is dominated by photoexcited/ionized plasmas, though in many cases photon statistics are not sufficient to draw firm conclusions (e.g., Sako et al. 2001, Kinkhabwala et al.

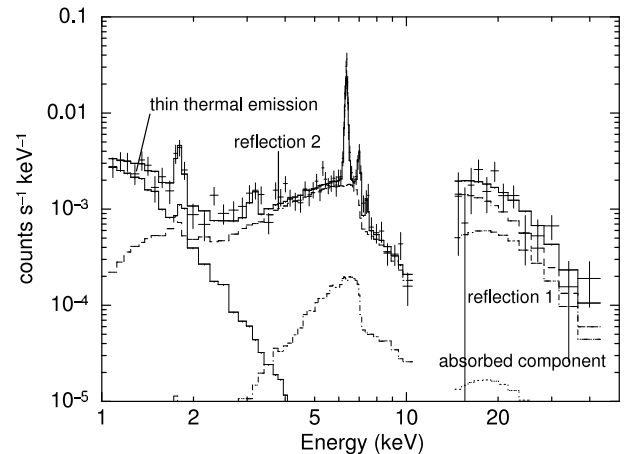


Fig. 4. *Suzaku* spectra of the Seyfert 2 NGC 2273 fitted with a combination of our simulation model, thin thermal plasma, and Gaussians. Absorbed reflection (reflection 1), unabsorbed reflection (reflection 2), and absorbed direct components are shown as dot-dashed, dashed, and dotted lines, respectively.

2002, Guainazzi et al. 2007). If we assume that the soft emission is primarily from X-rays scattered by photoionized gas, its strength relative to intrinsic X-ray emission (scattering fraction  $f_{\text{scat}}$ ) is expected to be proportional to the solid angle of the absorbing matter ( $\Delta\Omega$ ) and scattering optical depth ( $\tau$ ). Therefore, the weakness of soft X-ray emission implies that the opening part of the absorber is very small and that the central AGN is almost buried by a geometrically thick absorber. The most extreme case of buried AGNs in a *Swift*/BAT sample has been first reported by Ueda et al. (2007) and designated as a new type of AGNs because of their extremely small scattering fractions ( $< 0.5\%$ ). More examples of such a class of AGNs are then found (Eguchi et al. 2009; Winter et al. 2009a, b).

#### 5. Buried AGNs Found in the *XMM-Newton* Archives

After the discovery of the new type of buried AGNs in our *Swift*/BAT-*Suzaku* program, we tried to search for obscured AGNs with various value of scattering fraction from the *XMM-Newton* archives. The procedure and results are presented in Noguchi et al. (2009, 2010). We used hardness ratios listed in the second *XMM-Newton* serendipitous source catalogue (Watson et al. 2009) and selected candidates for obscured AGNs with  $N_H = 10^{23-24} \text{ cm}^{-2}$  covering a wide range of scattering fractions ( $f_{\text{scat}} = 0.1 - 10\%$ ). We analyzed their spectra made from the archival *XMM-Newton* data supplemented by some *Suzaku* data to quantitatively determine spectral parameters and  $f_{\text{scat}}$ , and constructed a sample of obscured AGNs consisting of 38 objects with  $N_H$  and  $f_{\text{scat}}$  in the above range.

If we assume that the scattering fraction reflects the

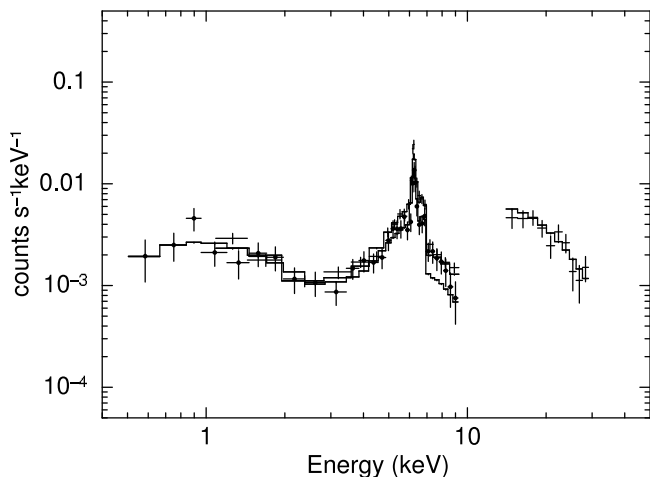


Fig. 5. *Suzaku* spectra of the *Swift*/BAT selected AGN ESO 506-G027 fitted with a model consisting of a partially covered power law, a reflection continuum, and a Gaussian.

solid angle of the opening part of the obscuring matter, our sample should contain obscured AGNs with various shape of the absorber. Objects with small scattering fraction are expected to have a small opening part of the absorber. Since optical narrow emission lines are emitted from the opening direction of the absorber, weaker optical lines at a given intrinsic power of the central source would be expected as predicted by Ueda et al. (2007). We therefore investigated a ratio of extinction-corrected [OIII] to absorption corrected 2–10 keV luminosities, and found that objects with small  $f_{\text{scat}}$  tend to show smaller ratios, which is exactly what we expected (see Figure 2 in Noguchi et al. 2010). This result suggests that selection based on optical narrow emission lines would be biased against obscured AGNs with a small opening part of obscuring matter.

## 6. Implications for Evolution

The formation and structure of obscuring matter around an AGN may be related to the amount of available gas and star formation activity around the nucleus. In an early stage of galaxy evolution, where active star formation is on going, it would be expected that nucleus is embedded in gas rich environment and that AGN is obscured by a large amount of gas and dust. Thus understanding the nature of highly obscured AGN population could have interesting implications to probe co-evolution of AGN and its host.

We used our sample of obscured AGN defined in the previous section to investigate relationships between scattering fractions and some fundamental parameters of the AGNs. The black hole masses  $M_{\text{BH}}$  were derived by using stellar velocity dispersion ( $\sigma$ ) taken from the literature and the  $M_{\text{BH}}-\sigma$  relation by Tremaine et al. (2002).

We found no significant correlation between  $M_{\text{BH}}$  and scattering fractions  $f_{\text{scat}}$ . We then calculated Eddington ratios (bolometric luminosity divided by Eddington luminosity  $L_{\text{bol}}/L_{\text{Edd}}$ ) and found a negative correlation between  $L_{\text{bol}}/L_{\text{Edd}}$  and  $f_{\text{scat}}$  (see Figure 3 in Noguchi et al. 2010). This relation implies that AGNs with small  $f_{\text{scat}}$  undergo extensive accretion and that a growth phase of central black hole could be highly obscured by geometrically thick obscuring matter.

I am grateful to my collaborators H. Awaki, S. Eguchi, R. Mushotzky, K. Noguchi, Y. Ueda, and L. Winter. This work is supported by Grants-in-Aid for Scientific Research (20740109) from the Ministry of Education, Culture, Sports, Science, and Technology of Japan.

## References

- Awaki H. et al. 1990 *Nature*, 346, 544
- Awaki H. et al. 2009 *PASJ.*, 61, S317
- Awaki H. et al. 2010 this volume
- Done C. et al. 1996 *ApJ.*, 463, L63
- Eguchi S. et al. 2009 *ApJ.*, 696, 1657
- Guainazzi M. & Bianchi S. 2007, *MNRAS*, 374, 1290
- Heckman T. M. et al. 2005 *ApJ.*, 634, 161
- Ikeda S. et al. 2009 *ApJ.*, 692, 608
- Kinkhabwala A. et al. 2002 *A&A.*, 575, 732
- Maiolino R. & Rieke G.H. 1995 *ApJ.*, 454, 95
- Markwardt C. et al. 2005 *ApJ.*, 633, L77
- Noguchi K. et al. 2009 *ApJ.*, 705, 454
- Noguchi K. et al. 2010 this volume
- Risaliti G. et al. 1999 *ApJ.*, 522, 157
- Sako M. et al. 2000, *ApJ.*, L115
- Tremaine S. et al. 2002, *ApJ.*, 574, 740
- Tueller J. et al. 2008, *ApJ.*, 681, 113
- Ueda Y. et al. 2007 *ApJ.*, 664, L79
- Watson M.G. et al. 2009 *A&A.*, 493, 339
- Winter L. et al. 2009a *ApJ.*, 690, 1322
- Winter L. et al. 2009b *ApJ.*, 701, 1644